Cooperative Interplay of van der Waals Forces and Quantum Nuclear Effects on Adsorption: H at Graphene and at Coronene

Erlend R. M. Davidson,[†,‡,§] Jiří Klimeš,[†,‡,§] Dario Alfè,[†,§,⊥,∥] and Angelos Michaelides[*,‡,†,§]

[†]London Centre for Nanotechnology, University College London, London WC1E 6BT, U.K., [‡]Department of Chemistry, University College London, London WC1E 6BT, U.K., [§]Thomas Young Centre, University College London, London WC1E 6BT, U.K., [⊥]Department of Earth Sciences, University College London, Gower Street, London, WC1E 6BT, U.K., and [∥]Department of Physics and Astronomy, University College London, London WC1E 6BT, U.K.

ABSTRACT The energetic barriers that atoms and molecules often experience when binding to surfaces are incredibly important to a myriad of chemical and physical processes. However, these barriers are difficult to describe accurately with current computer simulation approaches. Two prominent contemporary challenges faced by simulation are the role of van der Waals forces and nuclear quantum effects. Here we examine the widely studied model systems of hydrogen on graphene and coronene using a van der Waals inclusive density functional theory approach together with path integral molecular dynamics at 50 K. We find that both van der Waals and quantum nuclear effects work together in a cooperative manner to dramatically reduce the barriers for hydrogen atoms to adsorb. This suggests that the low temperature hydrogenation of graphene is easier than previously thought and in more general terms that the combined roles of van der Waals and quantum tunnelling can lead to qualitative changes in adsorption.

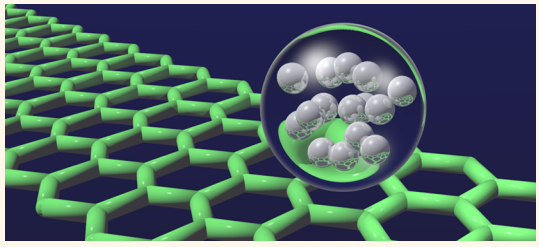

KEYWORDS: van der Waals forces · quantum nuclear effects · density functional theory · path integral molecular dynamics

The barriers that atoms and molecules experience when adsorbing or reacting on surfaces are directly relevant to an enormous number of chemical, physical, and technological processes. For example, bond making and bond breaking at metal and oxide surfaces lies at the heart of heterogeneous catalysis, photocatalysis, corrosion and nanoscale self-assembly. Likewise, adsorption and reaction on carbonaceous and siliceous surfaces is a critical step in the formation of molecules in the interstellar medium.

Adsorption barriers can be measured experimentally on well-defined atomically smooth surfaces with various techniques, including high precision molecular beam approaches.[1] From a simulation perspective, density functional theory (DFT) has become the method of choice for exploring bond making and bond breaking events at solid surfaces. Indeed DFT with standard generalized gradient approximation (GGA) functionals has been very successfully exploited to, *e.g.*, identify trends in heterogeneous catalysis.[2] Nonetheless standard GGAs used in most surface reactivity studies suffer from a number of shortcomings (see, *e.g.*, refs[3,4]). Not least among these is the neglect of van der Waals (vdW) dispersion forces. The omission of vdW forces in standard GGAs is an issue that has gained prominence recently and can be particularly important for adsorption, both in altering adsorption energies and in qualitatively changing the adsorption process.[5,6] Another issue with electronic structure simulations in general is that in the vast majority of them quantum nuclear effects (QNEs) (such as tunnelling and zero point motion) are not taken into account. Neglecting QNEs is a valid approximation in many circumstances; particularly for chemical reactions at surfaces of relevance to heterogeneous catalysis at high temperatures. However, at low temperature and for processes involving hydrogen QNEs become increasingly significant and should not be neglected (see, *e.g.*, refs[7,8]).

* Address correspondence to angelos.michaelides@ucl.ac.uk.

Received for review January 23, 2014 and accepted October 9, 2014.

Published online October 09, 2014
10.1021/nn505578x

© 2014 American Chemical Society

The classic low temperature adsorption process where QNEs can be expected to play a role is H adsorption on the surfaces of carbonaceous materials. Hydrogen adsorption on carbon based materials such as graphite and graphene is relevant to hydrogen storage,[9] band gap engineering,[10−13] and potentially as the first step in H_2 formation in the interstellar medium.[14−30] Although there is enormous interest in H adsorption on carbonaceous surfaces, with graphene, graphite and polycyclic aromatic hydrocarbons (PAHs) being the most widely studied model systems, we still do not fully understand the seemingly simple process of how a single H atom adsorbs on the surface. First, there are question marks over the energy barrier a H atom encounters upon adsorbing on the surface. The most well-defined experiment performed to date placed the barrier for H atom adsorption on graphite somewhere within the rather broad range of 25 to 250 meV.[31] Previous theoretical work on extended carbonaceous surfaces (graphite, and more commonly a single graphene layer) have been at the upper end of the experimental range (*ca.* 200 meV[16,19,32−35]). However, since they did not account for vdW forces and failed to capture the physisorbed H atom precursor state,[20,36] these previous theoretical determinations of the barrier must be treated with caution. Second, surprisingly little attention has been placed on the role quantum nuclear effects play in the adsorption process. Two notable exceptions are the recent graphene hydrogenation experiments of Paris *et al.*[37] and the quantum rate calculations of Goumans *et al.*[28,29] In the former a strong kinetic isotope effect for the adsorption of translationally hot hydrogen atoms on quasi-free-standing graphene was identified; the rate of uptake of deuterium being greater than that of hydrogen due to zero-point energy (ZPE) weakening the H−C bonds more than the D−C bonds. In the latter, quantum tunneling calculations were performed for the chemisorption of H at the edge sites of benzene and pyrene and an enhancement of the chemisorption rate at temperatures below ∼200 K was predicted.

It is clear that vdW and quantum nuclear effects are likely to be of importance to H atom chemisorption on carbonaceous surfaces and so here we address this head on with a combination of state of the art computer simulation approaches. For the treatment of vdW interactions, many schemes have recently been developed which could in principle be applied to this system (see, for example, ref[5]). Most results in the present manuscript have been obtained with the so-called "DFT-D3" functional (specifically PBE-D3),[38] however, the key results of our study are not particularly sensitive to the specific vdW scheme used and as we show in the Supporting Information the same conclusions are reached with the other vdW inclusive approaches. To account for quantum nuclear effects we use path integral based approaches, mainly *ab initio* path-integral molecular dynamics (PIMD) at a temperature of 50 K. *Ab initio* path-integral molecular dynamics (PIMD) is an approach which can accurately include thermal and quantum nuclear effects in complex systems involving bond-making and breaking by representing the quantum system by many classical replicas (called beads), which are connected by harmonic springs to form a ring-polymer. It is established as one of the most powerful schemes for considering zero-point energy (ZPE), quantum tunneling and delocalization of nuclei[39−41] and has been applied to a broad range of systems though not yet H at graphene.

Here we find that upon including dispersion the physisorption state for H on graphene is captured, which has been absent from previous studies, and the potential energy barrier to get to the chemisorbed state becomes narrower and lower. While accounting for quantum tunneling also increases the rate, this effect is strongly dependent on the shape of the underlying potential energy surface, especially on the width of the barrier. Consequently we find that dispersion effects vastly increase the rate constant of H atom tunneling to the chemisorption state. We show that this cooperative interplay applies to both H on graphene and at coronene, which is important for the specific systems considered as it provides a facile route to the chemisorbed H intermediate state in the formation of H_2 in the interstellar medium.[42] The results also suggest that the hydrogenation of graphene at low temperatures might be more facile than previously assumed and should depend strongly on the temperature and mass of the hydrogen atoms impinging on the surface. More generally, this study highlights the combined effect of dispersion and quantum nuclear effects on chemical reaction barriers, an effect that is likely to be relevant to a broad range of processes not just at surfaces but also, *e.g.*, in hydrogenation reactions in general and the formation of gas phase and bimolecular complexes.

RESULTS AND DISCUSSION

Hydrogen at Graphene. The focus of this study is low densities of H at carbonaceous surfaces, so we consider the adsorption of a single H atom in both the chemisorbed and physisorbed states. We discuss adsorption at the top site (directly above one carbon atom), since this is where chemisorption occurs, and the physisorption energies at the hollow, bridge and top sites are the same to within a few meV. The total energy profile using the standard Perdew−Burke−Ernzerhof (PBE) functional[43] is shown in Figure 1. As expected, and in agreement with many previous DFT GGA studies, the barrier between the gas phase and the chemisorbed state is about 200 meV.[16,19,32−35] The chemisorption well is 800 meV with a H−C bond length of 1.13 Å and puckering of the top site carbon atom away from the

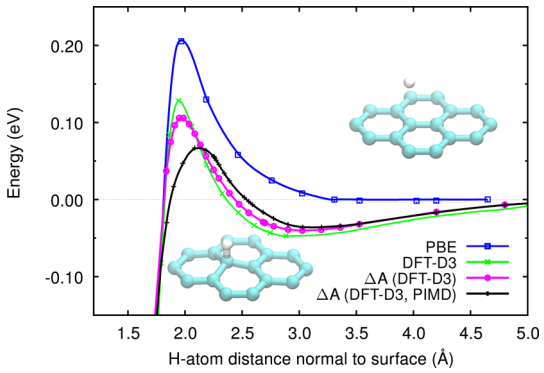

Figure 1. Energy profiles calculated with different approaches for the adsorption of a single H atom on graphene. The highest barrier (blue data) is the PBE potential energy barrier to chemisorption. Upon including vdW dispersion forces with DFT-D3 (green data) the potential energy barrier gets lower and narrower. The equivalent DFT-D3 free energy barrier (ΔA, pink data points) computed using *ab initio* MD at 50 K does not differ significantly from the underlying potential energy barrier. However, accounting for quantum nuclear effects with *ab initio* PIMD (black data) significantly lowers the free energy barrier. The H atom height above the surface is measured from the surface plane of the graphene sheet prior to chemisorption.

surface by ∼0.4 Å. With PBE there is no physisorption state, which is again consistent with previous work and understandable given the lack of a long-range correlation term in GGA exchange-correlation functionals.

Moving to DFT-D3 we find that there is indeed a physisorption state at a height of about 3.0 Å above the surface. The presence of a physisorbed state is consistent with calculations for H on PAHs[14,18,20,28,29,44] and experiments for H on graphite.[36] The depth of the physisorption well is approximately 47 meV and in very good agreement with the experimentally derived value for H on graphite of 40 meV.[36] The computed barrier to go from the physisorbed to the chemisorbed state (in this case relative to the bottom of the physisorption well) is reduced to about 175 meV and the depth of the chemisorption well increases to about 830 meV. In addition the barrier obtained with the vdW-inclusive DFT-D3 approach is narrower than that obtained with PBE. An overall lower and narrower barrier will increase the probability of a H atom chemisorbing on graphene by either thermal or quantum mechanical tunneling mechanisms. We will explore tunneling in detail below with path-integral methods but we can already assess how dispersion assists the tunneling process using the Wentzel−Kramers−Brillouin (WKB) approximation. In WKB the transmission coefficient, T, of a H atom of mass m_H though a barrier $V(z)$ between points a and b is given by

$$T \simeq \exp\left(-\frac{2}{\hbar}\int_a^b dz\sqrt{2m_H V(z)}\right) \qquad (1)$$

We find that using the PBE barrier yields $T \sim 10^{-8}$, whereas using the DFT-D3 barrier yields $T \sim 10^{-5}$. Thus, tunneling through the dispersion corrected barrier is expected to be much more facile than through the GGA barrier in which dispersion is neglected.

Previous theoretical studies of the chemisorption barrier of H at graphene have generally been static calculations of total energy at absolute zero, where the H atom is treated classically. Now we go beyond this by computing finite temperature free energy barriers for the H chemisorption process. Given the relevance of hydrogen adsorption to processes in the interstellar medium where temperatures are in the 10 to 100 K regime we have concentrated on a low temperature of 50 K. First, we computed the classical free energy profile for the chemisorption process; that is the free energy for the chemisorption of a classical hydrogen atom. Again this was done with the DFT-D3 functional and as can be seen in Figure 1 the free energy obtained is very similar to the underlying DFT-D3 potential energy profile: The physisorbed H state is virtually unchanged and the barrier to go from physisorption to chemisorption is smaller by about 23 meV (reduced from about 175 to about 152 meV). Next we computed the full quantum free energy profile for the chemisorption process with PIMD and a very pronounced difference emerged. In particular the quantum free energy barrier obtained from PIMD is only about 103 meV. This barrier, which includes vdW, ZPE effects, quantum tunneling and finite temperature effects, is approximately half the height of barriers typically predicted for H atom chemisorption at graphene using traditional DFT-GGA methods.[16,19,32−35] Although the barrier is substantially reduced the physisorption well remains relatively unperturbed, being a similar depth and shifted toward the gas phase by just ∼0.1 Å.

It is interesting to consider the separate roles of ZPE and quantum tunneling on the free energy barrier. Previous studies on other systems have found that the ZPE can be the dominant quantum nuclear effect.[45−49] Here we estimate the ZPE effects on the barrier by taking the difference between the sum of the real-valued vibrational frequencies at the transition state and in the physisorbed state. The ZPE in each state is computed using vibrational modes from the finite displacement method on the fully relaxed classical structure. This analysis reveals that ZPE effects actually increase the barrier by about 35 meV. Although this finding might appear surprising, it is to be expected since the lateral motion of the H atom becomes more constrained as it approaches the surface, and is consistent with previous calculations for H adsorption on pyrene.[29] This result is also consistent with the recent measurements from Paris *et al.*[37]

As ZPE cannot account for the reduced free energy barrier obtained from PIMD, it is constructive to consider how the H atom tunnels in more detail. To this end we start by examining the delocalization of the path-integral ring polymer at different heights above

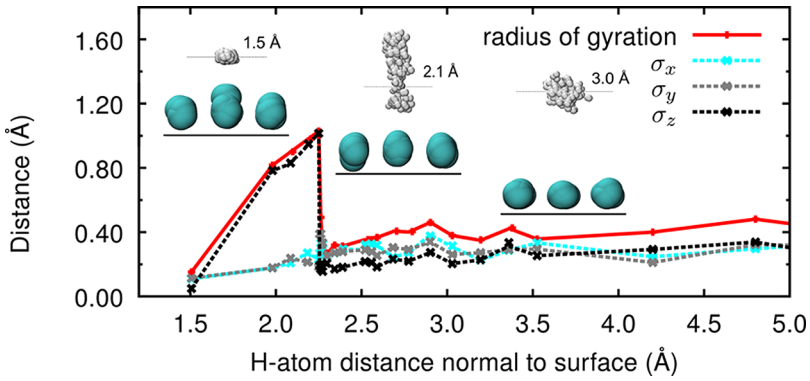

Figure 2. Radius of gyration for the path-integral ring-polymer as a function of the H atom distance from the surface. This is decomposed into lateral (*x*,*y*) and normal (*z*) components relative to the surface plane. Snapshots from calculations for the ring-polymer constrained close to the physisorption well at 3.0 Å, at the transition state at 2.1 Å, and unconstrained in the chemisorbed state at 1.5 Å above the graphene sheet. The snapshots are an aggregation of bead positions for several hundred steps. In the physisorption well the beads are only slightly more spread out in the direction of the surface normal than in the lateral directions. At the transition state there is much more broadening of the beads normal to the surface; some of the beads are chemisorbed while others are in the physisorbed state, and there is slight lateral squeezing of the beads at the height of the classical transition state. In the chemisorption well the beads are squeezed together due to the strong bonding with the surface.

the surface. This is done by computing the radius of gyration (R_{gyr}) of the ring-polymer at each point on the quantum free energy profile using the equation

$$(R_{gyr})^2 = \sum_{i=1}^{N} (\sigma_x^2 + \sigma_y^2 + \sigma_z^2) \qquad (2)$$

where N is the number of PIMD beads and σ_x, σ_y, σ_z are the standard deviations of the H atom beads in the x, y and z directions. Here we choose z to lie perpendicular to the surface, x and y lie parallel to the surface plane. This gives us a quantitative measure of the spread of the ring-polymer, and allows us to see the quantum character of the H atom as it approaches the barrier. As shown in Figure 2 at large H-graphene separations there is only a moderate spreading of the beads (R_{gyr} is about 0.4 Å). As the H atom approaches the surface the radius of gyration reduces very slightly because the particle feels the physisorption well. Upon approaching the classical saddle point (~2.1 Å) there is a dramatic increase in σ_z to 1.0 Å, due to spreading of the ring-polymer through the energy barrier toward the chemisorbed state. This indicates that the H is able to tunnel through the energy barrier toward the chemisorbed state. As the centroid is brought closer to the surface (<2 Å) the beads are compressed by the chemisorption well and the resultant formation of a strong H−C chemical bond. Snapshots of the aggregated bead positions obtained from the PIMD trajectories are also shown in Figure 2 for the H atom at a few selected heights. These simply show qualitatively the picture that has emerged from the analysis of the radius of gyration. Clearly the H atom is much "more quantum" in the physisorbed and transition state than in the chemisorbed state, due to the shape of the underlying potential. This is a very clear demonstration of how differences in quantum effects can occur for such relatively small geometric changes. In this case by simply moving the H atom ~1 Å closer to the surface from the physisorbed to the chemisorbed states the spread of the path-integral beads is reduced and the wave function of the H atom is localized.

TABLE 1. Summary of Some of the Key Properties for the Physisorption and Chemisorption of H at Graphene[a]

	PBE	DFT-D3	DFT-D3 (MD, 50 K)	DFT-D3 (PIMD, 50 K)
E_{phys} (meV)	0	47	47	36
barrier (meV)	203 [244]	175 [210]	152	103
κ (50 K)	10^{-21}	10^{-18}	10^{-16}	10^{-11}
$R^{phys-chem}$ (s^{-1})	—	~10^{-6}	~10^{-4}	~100

[a] E_{phys} is the energy of the physisorption well relative to a gas phase (desorbed) H atom. The barrier is reported relative to the physisorbed state or in the case of PBE, where there is no physisorbed state, to the gas phase (desorbed) H atom. Values in square brackets are corrected for ZPE. The equilibrium transition probability κ is computed from the Boltzmann factor (*i.e.*, $\exp(-\Delta E/k_B T)$) at 50 K. $R^{phys-chem}$ is the rate constant (per physisorbed H-atom) to go from the physisorbed to the chemisorbed state, computed from transition state theory at 50 K. The final column in which vdW and quantum effects are all taken in to consideration is the most accurate data reported in this article.

We now briefly consider how the reduction in chemisorption barrier affects the rate constant (per physisorbed H atom) of H chemisorption on the surface. Of course, there are many methods to compute transition rates (for example, refs[50,51]); however, here we are primarily interested in a qualitative understanding of the effects of dispersion and tunneling and so rely on a basic transition state theory approach.[69] From this we find that the chemisorption rate constant across the 50 K free energy barrier is ~10^{-4} s^{-1}, which increases to 100 s^{-1} when quantum nuclear effects are introduced *via* PIMD (Table 1). Thus, as we inferred from the WKB estimates, quantum tunneling

significantly increases the rate constant of adsorption in this system. This large increase in the rate constant for H chemisorption at graphene is comparable with the increase in rate constant observed in related studies on the edge sites of PAHs.[28,29] We note that the precise value for the rate constant of chemisorption depends also on the exchange-correlation functional used. However, as we show in the Supporting Information several vdW inclusive DFT approaches have been tested and they all show very significant increases in the rate constant; irrespective of the approach used, the combined inclusion of dispersion and quantum nuclear effects increases the likelihood of H atoms chemisorbing on graphene by many orders of magnitude.

Hydrogen at Polycyclic Aromatic Hydrocarbons (PAHs). The results of the last section point to a potentially general effect wherein vdW forces and quantum nuclear effects work together to significantly enhance the rate constant of H atom chemisorption. Here we demonstrate that the same physical effect is important to another closely related model system, namely, the adsorption of H on a PAH. As with graphene, PAHs are popular model systems for studying H adsorption on carbonaceous surfaces.[14,15,18,20,28,29,44,52−54] It is already known that quantum tunneling facilitates chemisorption at the outer edge sites of small PAHs;[29] however, an understanding of chemisorption at the core sites is vital in generalizing this to larger PAHs and carbonaceous materials. Here we compute the barrier for a H atom to chemisorb at one of the core C atoms of coronene again using the PBE and DFT-D3 functionals. Overall the results obtained are qualitatively similar to those on graphene. With PBE there is a chemisorption barrier of about 230 meV and no physisorption well. When vdW forces are accounted for at the PBE-D3 level a 43 meV physisorption well emerges at 3.0 Å from the lateral plane of the coronene molecule and the chemisorption barrier is reduced to 200 meV (relative to the physisorption state). Again, as well as being smaller we also find that the DFT-D3 chemisorption barrier is narrower than the PBE barrier.

To include quantum nuclear effects on this system we use the harmonic quantum transition state theory (HQTST) method (also known as instanton) on an analytical one-dimensional potential fitted to the underlying potential from DFT-D3. This is an alternative and more economical Feynman path-integral based method, which computes quantum tunneling by the spread of beads over the barrier. The beads spread into the wells either side of the potential barrier to lower their energy, which is in competition with the mass and temperature dependent springs that connect the beads in a ring-polymer. Using instanton theory for H adsorption on graphene yields a quantum energy barrier of ∼50 meV (Figure 3(a)). This is smaller than the quantum free energy barrier

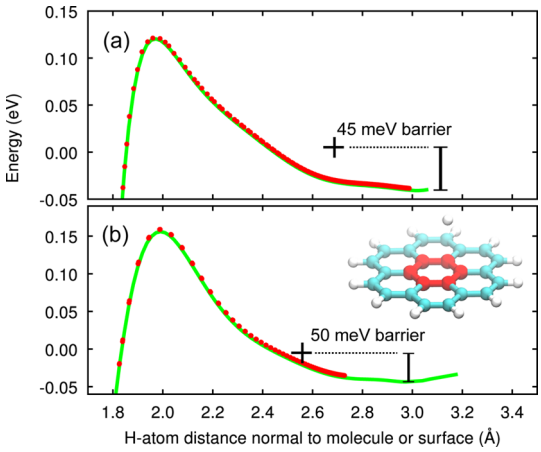

Figure 3. Plots of the heights and energies of the path-integral beads from instanton (HQTST) calculations at 50 K for H at graphene (a) and coronene (b). The solid green lines show the fit to the underlying DFT-D3 potential energy curves. The instanton path-integral beads are shown as red dots. The average of these beads (the centroid, shown as a black cross) gives the free energy barrier. The structure of the H/coronene adsorption system is shown in (b) where the red carbon atoms represent core atoms, which is where we consider the H chemisorption in this work.

obtained from for PIMD for H on graphene. However, once again we see that tunnelling leads to a major reduction in the effective barrier to chemisorption and instanton theory is able to qualitatively capture this effect. The results from the instanton calculation of H at coronene (Figure 3(b)) reveal a picture similar to the one that emerged on graphene: the quantum free energy barrier is about 50 meV relative to the physisorption well, substantially lower than the 200 meV potential energy barrier (including dispersion). Thus, on a PAH, as well as on graphene, quantum effects and dispersion dramatically increase the probability of covalent C−H bond formation at low temperatures.

CONCLUSIONS

With a view to understanding the combined role of vdW forces and quantum nuclear effects during the formation of a chemical bond at a solid surface, we have applied various state of the art simulation methods to better understand H chemisorption. This has led to the striking result that quantum nuclear effects and dispersion work together to dramatically increase the likelihood of H atoms chemisorbing on graphene and also at the core sites of PAHs. This shows that the role of quantum nuclear effects in the hydrogenation of carbonaceous surfaces is much greater than previously thought. A proper account of quantum nuclear effects yields a significantly lower free energy barrier to H chemisorption and our analysis reveals that this is due to quantum tunneling since ZPE effects actually slightly increase the chemisorption barrier. The use of PIMD in particular has enabled us to examine in detail the quantum nature of the H atom

as it approaches the surface, revealing that the quantum behavior of a H atom changes dramatically at different heights above the surface. This is most clearly seen in Figure 2 where we see that upon approaching the surface the H goes from being quantum mechanically spread out in the physisorbed state to being highly localized in the chemisorbed state, *via* the classical saddle point where the H atom spreads out by about 1 Å normal to the surface. Clearly the location of a particle at a surface has a direct effect on the amount of quantum mechanical spread, hence the importance of a quantum mechanical description of the system.

In this study we have gone beyond the standard GGA (PBE) description of H atom adsorption by making use of the DFT-D3 exchange-correlation functional.[38] Results from other vdW inclusive approaches are included in the Supporting Information, which also predict a reduction in the adsorption barrier, as did a recent study for H adsorption on coronene with the DFT-D3 approach.[14] The particular functional used here is a good choice for this system because it yields a physisorption well depth of 47 meV on graphene; close to the experimentally derived value of of 40 meV for H on graphite.[36] It also yields a physisorption energy of 43 meV on coronene, which falls on top of the reference second order Møller−Plesset perturbation theory (MP2) and diffusion quantum Monte Carlo (DMC) values of *ca*. 40 meV.[18,20] However, we caution that this level of agreement is to some extent fortuitous since: (i) DFT-D3 is an approximate method[5] and our calculations with other vdW-inclusive functionals reveal that the depth of the physisorption well is sensitive to the particular approach employed (see the Supporting Information); and (ii) the experimentally determined value for the physisorption energy is likely to have a large error bar since in the measurements only modest vacuum levels were employed and modern standards of ultrahigh vacuum cleanliness will not have been obtained.[36] Thus, although we have made progress and addressed some of the key shortcomings of previous electronic structure work performed on this system this is certainly not the end of the line as far as theory is concerned and it remains to be seen how close DFT-D3 comes to the "exact" potential energy barrier for H adsorption on graphene. Although it is possible to get reference binding energies for gas phase complexes (such as has been done recently for H on some small PAHs[20,55]), obtaining "beyond" DFT values for adsorption and reaction at extended surfaces remains a major challenge.[5] While it is beyond the scope of the current study, in the future it would be interesting to examine additional issues that might be relevant to the chemisorption barrier such as, *e.g.*, the potential role of exact exchange and beyond pairwise dispersion effects. Addressing these issues could involve the application DMC and/or the random phase approximation; two approaches that can be applied to adsorption on solids (with periodic boundary conditions). In addition it is worth noting that here we have considered the barrier to go from the physisorbed state to chemisorption, which implies that the H atom has time to equilibrate with the surface. A direct chemisorption process is also possible, whereby an incident gas phase H atom goes directly to the chemisorbed state. Examining such a process and any electronic excitations that might be associated with it would also make interesting work for the future.

Aside from theory, there is also scope for improving our experimental understanding of this system. First, a measurement of the H atom physisorption energy on graphene under ultra high vacuum conditions would be highly informative and provide an important benchmark for theory. Second, and more interesting, would be a set of molecular beam studies of H and D atom chemisorption on graphene specifically aimed at determining the temperature and isotope dependent rate of adsorption. Recently, in an elegant set of experiments on quasi free-standing graphene it was shown that D adsorption was more facile than H adsorption.[37] The H and D atoms were obtained with the standard approach of thermally cracking molecular hydrogen at very high temperatures (3000 K). As a result the H/D atoms impinging on the surface were translationally hot and at a much higher temperature than the graphene substrate; consequently in these measurements the high temperature limit of the chemisorption barrier will have been probed. The heavier mass of D (compared to H) results in its desorption barrier being higher, due to the lower ZPE level for D. Furthermore, if the H/D atoms cool down quickly after chemisorption at graphene, this effect will be compounded by the more rapid tunnelling of H through the top of the desorption barrier. This implies that at some intermediate temperature there will be a switchover in the relative rates of H and D adsorption on graphene. It is a major challenge to produce beams of H and D atoms with low kinetic energy−the lowest energy beams applied to this type of systems so far has been the 25 meV (∼300 K) source of Arèou *et al.*[31] However, new measurements with translationally cold H and D atoms down to temperatures of 50−150 K could test our suggestion of a temperature dependent switch in kinetic isotope effect, and would serve as a more realistic model for the ISM conditions.

Our results suggest that at low temperatures the chemisorption of a first H at carbonaceous materials is easier than previously thought. Scanning-tunnelling microscopy and DFT studies by Hornekær *et al.*[16] and Rougeau *et al.*[33] determined that once a single H atom has chemisorbed the barrier for subsequent H atoms

to chemisorb locally is much smaller. Considered in concert with our findings this therefore facilitates the low temperature hydrogenation of large regions of graphene. Given the strong temperature dependence in the relative rate of H and D adsorption suggested here, delicate isotopic control of this process may also be achievable.

Finally, our results relate directly to H adsorption on carbonaceous surfaces, however the interplay mechanism we propose between vdW and quantum tunnelling will likely apply to a variety of surface adsorption systems involving hydrogen. Indeed this work outlines the general necessity to use a combined quantum mechanical and dispersion treatment for surface processes involving H. Accounting for both of these effects has only become possible in recent years due to the development of vdW inclusive DFT methods and the advances in computational resources for large *ab initio* PIMD simulations. It remains to be seen for how many other chemical reactions a synergistic interplay of dispersion and quantum nuclear effects will play such an important role.

METHODS

The DFT calculations presented here used the VASP[56,57] code. This includes our own modifications[58] for PIMD,[48,59,60] which uses forces computed on-the-fly from the electronic structure calculations. Here we report results using PBE[43] and the DFT-D3[38] exchange-correlation functionals. The latter is a scheme for treating vdW forces in DFT through the inclusion on an additional C_6/R^6 term, where the C_6 dictates the strength of the binding and R is the distance between pairs of atoms. In the Supporting Information results from various nonlocal van der Waals density functionals[61−63] are reported. The main finding of this other work is that although the precise value of the barrier differs between the various approaches, the conclusion that dispersion brings the barrier down below that predicted by PBE remains unchanged.

Projector augmented wave (PAW) potentials[64] and a plane-wave basis set were used with periodic supercells and a cutoff energy of 450 eV. For graphene we used a 3×3 unit cell with a $5 \times 5 \times 1$ **k**-point mesh, and tests were performed on larger cells (see Supporting Information). Coronene was computed in a 15 Å cubic cell with a single (Γ) **k**-point. Since methods based on semilocal exchange are known to underestimate reaction barriers, due to self-interaction errors, we used the Heyd, Scuseria and Ernzerhof (HSE) screened Coulomb hybrid exchange-correlation functional[65] to test the height of the barrier for the H at coronene system. HSE gives a chemisorption barrier of approximately 250 meV, only 20 meV higher than the PBE value, suggesting that self-interaction errors may not be very large.

Total energy curves and minimum energy path (MEP) calculations used the climbing image nudged elastic band (CI-NEB) method.[66] Finite temperature effects were accounted for by *ab initio* molecular dynamics (MD) at 50 K, with the forces computed on the fly from DFT. The (constant volume) free energy profile along a normal incidence reaction coordinate for a H atom to go from 5 Å above the surface to chemisorption was obtained using the potential of mean force (PMF) method. In this method the H is constrained at several heights above the surface and for each height the component of force normal to the surface is averaged over a sufficient number of MD steps to obtain a converged average value (generally upward of 1000 steps were required). These average forces are then integrated to give the free energy barrier. Quantum nuclear effects are accounted for by the same PMF method with the height constraint placed on the centroid of the PIMD ring-polymer.[48,60,67] All the dynamics simulations are propagated with the velocity-Verlet scheme, and the temperature is controlled using a Nosé−Hoover chain thermostat for the MD and a Langevin thermostat for the PIMD. A time-step of 0.3 fs is used in both the MD and PIMD simulations, although it must be emphasized that within the PIMD scheme MD is used purely for sampling and so the time-steps do not map on to any physical time domain. Our PIMD simulations used 16 imaginary time-slices (beads), which is a reasonable compromise between accuracy and computational tractability (see Supporting Information). We also made use of the HQTST method (also called instanton)[68] on analytical potentials which have been fitted to the underlying DFT potential energy surface. These calculations used a total of 200 beads.

Conflict of Interest: The authors declare no competing financial interest.

Acknowledgment. Some of the research leading to these results has received funding from the European Research Council under the European Union's Seventh Framework Programme (FP/2007-2013)/ERC Grant Agreement No. 616121 (Heterolce project) and the Royal Society through a Wolfson Research merit Award (A. M.). D. A. is also supported through the Royal Society Wolfson Research Merit Award and EPSRC. This research used resources of the Oak Ridge Leadership Computing Facility, located in the National Center for Computational Sciences at Oak Ridge National Laboratory, which is supported by the Office of Science of the Department of Energy under Contract No. DE-AC05-00OR22725. We are also grateful for computational resources to the London Centre for Nanotechnology and UCL Research Computing for providing the Legion@UCL service. Finally we are grateful as well to the UK's HPC Materials Chemistry Consortium, which is funded by EPSRC (EP/F067496), for access to HECToR, the UK's national high-performance computing service.

Supporting Information Available: H atom physisorption energy and chemisorption barrier for different exchange-correlation functionals and cell sizes. Convergence of the number of beads used in the harmonic quantum transition state theory calculations and convergence of the number of beads used in the path-integral molecular dynamics simulations. This material is available free of charge *via* the Internet at http://pubs.acs.org.

REFERENCES AND NOTES

1. Somorjai, G. A.; Li, Y. *Surface Chemistry and Catalysis*; John Wiley & Sons: New York, 2010.
2. Nørskov, J. K.; Bligaard, T.; Rossmeisl, J.; Christensen, C. H. Towards the Computational Design of Solid Catalysts. *Nat. Chem.* **2009**, *1*, 37.
3. Cohen, A. J.; Mori-Sánchez, P.; Yang, W. Insights into Current Limitations of Density Functional Theory. *Science* **2008**, *321*, 792.
4. Burke, K. Perspective on Density Functional Theory. *J. Chem. Phys.* **2012**, *136*, 150901.
5. Klimeš, J.; Michaelides, A. Perspective: Advances and Challenges in Treating van der Waals Dispersion Forces in Density Functional Theory. *J. Chem. Phys.* **2012**, *137*, 120901.
6. Liu, W.; Filimonov, S. N.; Carrasco, J.; Tkatchenko, A. Molecular Switches from Benzene Derivatives Adsorbed on Metal Surfaces. *Nat. Commun.* **2013**, *4*, 2569.
7. Jewell, A. D.; Peng, G.; Mattera, M. F. G.; Lewis, E. A.; Murphy, C. J.; Kyriakou, G.; Mavrikakis, M.; Sykes, E. C. H. Quantum

Tunneling Enabled Self-Assembly of Hydrogen Atoms on Cu(111). *ACS Nano* **2012**, *6*, 10115.
8. McIntosh, E. M.; Wikfeldt, K. T.; Ellis, J.; Michaelides, A.; Allison, W. Quantum Effects in the Diffusion of Hydrogen on Ru (0001). *J. Phys. Chem. Lett.* **2013**, *4*, 1565.
9. Schlapbach, L.; Zuttel, A. Hydrogen-Storage Materials for Mobile Applications. *Nature* **2001**, *414*, 353–358.
10. Elias, D. C.; Nair, R. R.; Mohiuddin, T. M. G.; Morozov, S. V.; Blake, P.; Halsall, M. P.; Ferrari, A. C.; Boukhvalov, D. W.; Katsnelson, M. I.; Geim, A. K.; Novoselov, K. S.; *et al.* Control of Graphene's Properties by Reversible Hydrogenation: Evidence for Graphane. *Science* **2009**, *323*, 610–613.
11. Haberer, D.; Vyalikh, D. V.; Taioli, S.; Dora, B.; Farjam, M.; Fink, J.; Marchenko, D.; Pichler, T.; Ziegler, K.; Simonucci, S.; *et al.* Tunable Band Gap in Hydrogenated Quasi-Free-Standing Graphene. *Nano Lett.* **2010**, *10*, 3360.
12. Balog, R.; Jørgensen, B.; Nilsson, L.; Andersen, M.; Rienks, E.; Bianchi, M.; Fanetti, M.; Lægsgaard, E.; Baraldi, A.; Lizzit, S.; *et al.* Bandgap Opening in Graphene Induced by Patterned Hydrogen Adsorption. *Nat. Mater.* **2010**, *9*, 315–319.
13. Bostwick, A.; McChesney, J. L.; Emtsev, K. V.; Seyller, T.; Horn, K.; Kevan, S. D.; Rotenberg, E. Quasiparticle Transformation During a Metal-Insulator Transition in Graphene. *Phys. Rev. Lett.* **2009**, *103*, 056404.
14. Rougeau, N.; Teillet-Billy, D.; Sidis, V. On the PES for the Interaction of an H Atom with an H Chemisorbate on a Graphenic Platelet. *Phys. Chem. Chem. Phys.* **2011**, *13*, 17579–17587.
15. Bonfanti, M.; Casolo, S.; Tantardini, G. F.; Martinazzo, R. Surface Models and Reaction Barrier in Eley-Rideal Formation of H(2) on Graphitic Surfaces. *Phys. Chem. Chem. Phys.* **2011**, *13*, 16680–16688.
16. Hornekær, L.; Rauls, E.; Xu, W.; Šljivančanin, Z.; Otero, R.; Stensgaard, I.; Lægsgaard, E.; Hammer, B.; Besenbacher, F. Clustering of Chemisorbed H(D) Atoms on the Graphite (0001) Surface Due to Preferential Sticking. *Phys. Rev. Lett.* **2006**, *97*, 186102.
17. Hornekær, L.; Šljivančanin, Z.; Xu, W.; Otero, R.; Rauls, E.; Stensgaard, I.; Lægsgaard, E.; Hammer, B.; Besenbacher, F. Metastable Structures and Recombination Pathways for Atomic Hydrogen on the Graphite (0001) Surface. *Phys. Rev. Lett.* **2006**, *96*, 156104.
18. Bonfanti, M.; Martinazzo, R.; Tantardini, G. F.; Ponti, A. Physisorption and Diffusion of Hydrogen Atoms on Graphite from Correlated Calculations on the H-Coronene Model System. *J. Phys. Chem. C* **2007**, *111*, 5825–5829.
19. Ivanovskaya, V. V.; Zobelli, A.; Teillet-Billy, D.; Rougeau, N.; Sidis, V.; Briddon, P. R. Hydrogen Adsorption on Graphene: A First Principles Study. *Eur. Phys. J. B* **2010**, *76*, 481–486.
20. Ma, J.; Michaelides, A.; Alfè, D. Binding of Hydrogen on Benzene, Coronene, and Graphene from Quantum Monte Carlo Calculations. *J. Chem. Phys.* **2011**, *134*, 134701.
21. Hirama, M.; Ishida, T.; Aihara, J. I. Possible Molecular Hydrogen Formation Mediated by the Radical Cations of Anthracene and Pyrene. *J. Comput. Chem.* **2003**, *24*, 1378–1382.
22. Ferullo, R. M.; Domancich, N. F.; Castellani, N. J. On the Performance of van der Waals Corrected-Density Functional Theory in Describing the Atomic Hydrogen Physisorption on Graphite. *Chem. Phys. Lett.* **2010**, *500*, 283–286.
23. Williams, D. A.; Williams, D. E.; Clary, D. C.; Farebrother, A.; Fisher, A.; Gingell, J.; Jackman, R.; Mason, N.; Meijer, A.; Perry, J. *et al.* In *Molecular Hydrogen in Space*; Combes, F., DesForets, G. P., Eds.; Cambridge Contemporary Astrophysics, Cambridge University Press: Cambridge, U.K., 2000; pp 99−106.
24. Ehrenfreund, P.; Fraser, H. J.; Blum, J.; Cartwright, J. H. E.; García-Ruiz, J. M.; Hadamcik, E.; Levasseur-Regourd, A. C.; Price, S.; Prodi, F.; Sarkissian, A. Physics and Chemistry of Icy Particles in the Universe: Answers from Microgravity. *Planet. Space Sci.* **2003**, *51*, 473–494.
25. Meijer, A. J. H. M.; Farebrother, A. J.; Clary, D. C.; Fisher, A. J. Time-Dependent Quantum Mechanical Calculations on the Formation of Molecular Hydrogen on a Graphite Surface *via* an Eley-Rideal Mechanism. *J. Phys. Chem. A* **2001**, *105*, 2173–2182.
26. Meijer, A. J. H. M.; Farebrother, A. J.; Clary, D. C. Isotope Effects in the Formation of Molecular Hydrogen on a Graphite Surface *via* an Eley-Rideal Mechanism. *J. Phys. Chem. A* **2002**, *106*, 8996–9008.
27. Meijer, A. J. H. M.; Fisher, A. J.; Clary, D. C. Surface Coverage Effects on the Formation of Molecular Hydrogen on a Graphite Surface *via* an Eley-Rideal Mechanism. *J. Phys. Chem. A* **2003**, *107*, 10862–10871.
28. Goumans, T. P. M.; Kastner, J. Hydrogen-Atom Tunneling Could Contribute to H-2 Formation in Space. *Angew. Chem., Int. Ed.* **2010**, *49*, 7350–7352.
29. Goumans, T. P. M. Hydrogen Chemisorption on Polycyclic Aromatic Hydrocarbons *via* Tunnelling. *Mon. Not. R. Astron. Soc.* **2011**, *415*, 3129–3134.
30. Iqbal, W.; Acharyya, K.; Herbst, E. Kinetic Monte Carlo Studies of H-2 Formation on Grain Surfaces over a Wide Temperature Range. *Astrophys. J.* **2012**, *751*, 58.
31. Aréou, E.; Cartry, G.; Layet, J. M.; Angot, T. Hydrogen-Graphite Interaction: Experimental Evidences of an Adsorption Barrier. *J. Chem. Phys.* **2011**, *134*, 014701.
32. Sha, X. W.; Jackson, B. First-Principles Study of the Structural and Energetic Properties of H Atoms on a Graphite (0001) Surface. *Surf. Sci.* **2002**, *496*, 318–330.
33. Rougeau, N.; Teillet-Billy, D.; Sidis, V. Double H Atom Adsorption on a Cluster Model of a Graphite Surface. *Chem. Phys. Lett.* **2006**, *431*, 135–138.
34. Šljivančanin, Z.; Rauls, E.; Hornekær, L.; Xu, W.; Besenbacher, F.; Hammer, B. Extended Atomic Hydrogen Dimer Configurations on the Graphite(0001) Surface. *J. Chem. Phys.* **2009**, *131*, 084706.
35. Sha, X. W.; Jackson, B.; Lemoine, D. Quantum Studies of Eley-Rideal Reactions Between H Atoms on a Graphite Surface. *J. Chem. Phys.* **2002**, *116*, 7158–7169.
36. Ghio, E.; Mattera, L.; Salvo, C.; Tommasini, F.; Valbusa, U. Vibrational-Spectrum of H and D on the (0001) Graphite Surface from Scattering Experiments. *J. Chem. Phys.* **1980**, *73*, 556–561.
37. Paris, A.; Verbitskiy, N.; Nefedov, A.; Wang, Y.; Fedorov, A.; Haberer, D.; Oehzelt, M.; Petaccia, L.; Usachov, D.; Vyalikh, D.; *et al.* Kinetic Isotope Effect in the Hydrogenation and Deuteration of Graphene. *Adv. Funct. Mater.* **2013**, *23*, 1628.
38. Grimme, S.; Antony, J.; Ehrlich, S.; Krieg, H. A Consistent and Accurate *Ab Initio* Parametrization of Density Functional Dispersion Correction (DFT-D) for the 94 Elements H-Pu. *J. Chem. Phys.* **2010**, *132*, 154104.
39. Tuckerman, M. E.; Marx, D. Heavy-Atom Skeleton Quantization and Proton Tunneling in "Intermediate-Barrier" Hydrogen Bonds. *Phys. Rev. Lett.* **2001**, *86*, 4946–4949.
40. Braams, B. J.; Manolopoulos, D. E. On the Short-Time Limit of Ring Polymer Molecular Dynamics. *J. Chem. Phys.* **2006**, *125*, 124105.
41. Li, X. Z.; Walker, B.; Michaelides, A. Quantum Nature of the Hydrogen Bond. *Proc. Natl. Acad. Sci. U. S. A.* **2011**, *108*, 6369–6373.
42. Cazaux, S.; Tielens, A. G. G. M. Formation on Grain Surfaces. *Astrophys. J.* **2004**, *604*, 222–237.
43. Perdew, J. P.; Burke, K.; Ernzerhof, M. Generalized Gradient Approximation Made Simple. *Phys. Rev. Lett.* **1996**, *77*, 3865–3868.
44. Ferullo, R. M.; Domancich, N. F.; Castellani, N. J. On the Performance of van der Waals Corrected-Density Functional Theory in Describing the Atomic Hydrogen Physisorption on Graphite. *Chem. Phys. Lett.* **2010**, *500*, 283–286.
45. Walker, B.; Michaelides, A. Direct Assessment of Quantum Nuclear Effects on Hydrogen Bond Strength by Constrained-Centroid *Ab Initio* Path Integral Molecular Dynamics. *J. Chem. Phys.* **2010**, *133*, 174306.
46. Ando, K.; Hynes, J. T. Molecular Mechanism of HCl Acid Ionization in Water: *Ab Initio* Potential Energy Surfaces and Monte Carlo Simulations. *J. Phys. Chem. B* **1997**, *101*, 10464–10478.

47. Marx, D.; Tuckerman, M. E.; Hutter, J.; Parrinello, M. The Nature of the Hydrated Excess Proton in Water. *Nature* **1999**, *397*, 601–604.
48. Tuckerman, M. E.; Marx, D.; Klein, M. L.; Parrinello, M. On the Quantum Nature of the Shared Proton in Hydrogen Bonds. *Science* **1997**, *275*, 817–820.
49. Kumagai, T.; Kaizu, M.; Okuyama, H.; Hatta, S.; Aruga, T.; Hamada, I.; Morikawa, Y. Symmetric Hydrogen Bond in a Water-Hydroxyl Complex on Cu(110). *Phys. Rev. B: Condens. Matter Mater. Phys.* **2010**, *81*, 045402.
50. Truhlar, D. G.; Garrett, B. C. Variational Transition-State Theory. *Acc. Chem. Res.* **1980**, *13*, 440–448.
51. Dellago, C.; Bolhuis, P. G.; Csajka, F. S.; Chandler, D. Transition Path Sampling and the Calculation of Rate Constants. *J. Chem. Phys.* **1998**, *108*, 1964–1977.
52. Jeloaica, L.; Sidis, V. DFT Investigation of the Adsorption of Atomic Hydrogen on a Cluster-Model Graphite Surface. *Chem. Phys. Lett.* **1999**, *300*, 157–162.
53. Ivanovskaya, V. V.; Zobelli, A.; Teillet-Billy, D.; Rougeau, N.; Sidis, V.; Briddon, P. R. Enhanced H(2) Catalytic Formation on Specific Topological Defects in Interstellar Graphenic Dust Grain Models. *Phys. Rev. B: Condens. Matter Mater. Phys.* **2010**, *82*, 245407.
54. Rauls, E.; Hornekaer, L. Catalyzed Routes to Molecular Hydrogen Formation and Hydrogen Addition Reactions on Neutral Polycyclic Aromatic Hydrocarbons Under Interstellar Conditions. *Astrophys. J.* **2008**, *679*, 531–536.
55. Wang, Y.; Qian, H.-J.; Morokuma, K.; Irle, S. Coupled Cluster and Density Functional Theory Calculations of Atomic Hydrogen Chemisorption on Pyrene and Coronene As Model Systems for Graphene Hydrogenation. *J. Phys. Chem. A* **2012**, *116*, 7154.
56. Kresse, G.; Furthmüller, J. Efficiency of *Ab-Initio* Total Energy Calculations for Metals and Semiconductors Using a Plane-Wave Basis Set. *Comput. Mater. Sci.* **1996**, *6*, 15–50.
57. Kresse, G.; Furthmüller, J. Efficient Iterative Schemes for *Ab Initio* Total-Energy Calculations Using a Plane-Wave Basis Set. *Phys. Rev. B: Condens. Matter Mater. Phys.* **1996**, *54*, 11169–11186.
58. Alfè, D.; Gillan, M. J. *Ab Initio* Statistical Mechanics of Surface Adsorption and Desorption. II. Nuclear Quantum Effects. *J. Chem. Phys.* **2010**, *133*, 044103.
59. Marx, D.; Parrinello, M. *Ab-Initio* Path-Integral Molecular-Dynamics. *Z. Phys. B: Condens. Matter* **1994**, *95*, 143–144.
60. Marx, D.; Parrinello, M. Structural Quantum Effects and 3-Center 2-Electron Bonding in CH5+. *Nature* **1995**, *375*, 216–218.
61. Dion, M.; Rydberg, H.; Schröder, E.; Langreth, D. C.; Lundqvist, B. I. Van der Waals Density Functional for General Geometries. *Phys. Rev. Lett.* **2004**, *92*, 246401.
62. Klimeš, J.; Bowler, D. R.; Michaelides, A. Chemical Accuracy for the van der Waals Density Functional. *J. Phys.: Condens. Matter* **2010**, *22*, 022201.
63. Klimeš, J.; Bowler, D. R.; Michaelides, A. Van der Waals Density Functionals Applied to Solids. *Phys. Rev. B: Condens. Matter Mater. Phys.* **2011**, *83*, 195131.
64. Blöchl, P. E. Projector Augmented-Wave Method. *Phys. Rev. B: Condens. Matter Mater. Phys.* **1994**, *50*, 17953–17979.
65. Heyd, J.; Scuseria, G. E.; Ernzerhof, M. Hybrid Functionals Based on a Screened Coulomb Potential. *J. Chem. Phys.* **2003**, *118*, 8207–8215.
66. Henkelman, G.; Uberuaga, B. P.; Jónsson, H. A Climbing Image Nudged Elastic Band Method for Finding Saddle Points and Minimum Energy Paths. *J. Chem. Phys.* **2000**, *113*, 9901–9904.
67. Gillan, M. J. Quantum-Classical Crossover of the Transition Rate in the Damped Double Well. *J. Phys. C* **1987**, *20*, 3621.
68. Arnaldsson, A. Ph.D. thesis, University of Washington, Seattle, WA, 2007.
69. For the potential energy barriers ΔE we use the expression $R^{\mathrm{phys-chem}} = A \exp(-\Delta E/k_B T)$ where the prefactor $A(\sim 10^{13})\ s^{-1}$ is computed by taking a ratio of the product of frequencies at the initial (physisorbed) state with the product of frequencies at the transition state, within the harmonic approximation. No rate is reported for PBE since there is no physisorption state for the H atom and so no initial state frequency along the reaction coordinate. For the free energy barriers we compute the rate from $R^{\mathrm{phys-chem}} = \kappa_\alpha \exp(-\Delta F k_B T)$, where the attempt frequency $\kappa_\alpha(\sim 10^{12})\ s^{-1}$ is the vibrational mode of the physisorbed H acting along the reaction coordinate.